Accepted Manuscript

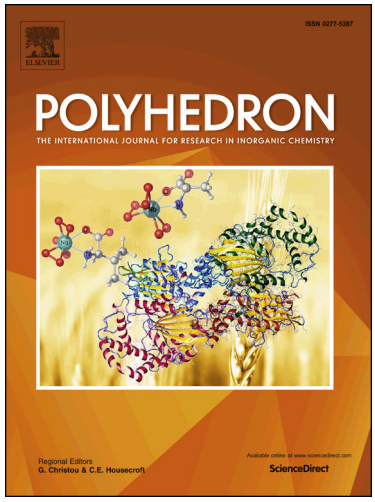

Cu(I) coordination polymer based on pyridyl-functionalized resorcinarene: selective detection of $Cr_2O_7^{2-}$, MnO_4^- and nitrobenzene and efficient catalyst for azide-alkyne cycloaddition reaction

Yan-Li Liu, Lei Yan, Ying-Ying Liu, Guo-Hai Xu, Wen-Jing Shi, Jian-Fang Ma

PII: S0277-5387(18)30757-5
DOI: https://doi.org/10.1016/j.poly.2018.11.032
Reference: POLY 13579

To appear in: *Polyhedron*

Received Date: 2 October 2018
Accepted Date: 11 November 2018

Please cite this article as: Y-L. Liu, L. Yan, Y-Y. Liu, G-H. Xu, W-J. Shi, J-F. Ma, Cu(I) coordination polymer based on pyridyl-functionalized resorcinarene: selective detection of $Cr_2O_7^{2-}$, MnO_4^- and nitrobenzene and efficient catalyst for azide-alkyne cycloaddition reaction, *Polyhedron* (2018), doi: https://doi.org/10.1016/j.poly.2018.11.032

This is a PDF file of an unedited manuscript that has been accepted for publication. As a service to our customers we are providing this early version of the manuscript. The manuscript will undergo copyediting, typesetting, and review of the resulting proof before it is published in its final form. Please note that during the production process errors may be discovered which could affect the content, and all legal disclaimers that apply to the journal pertain.

Cu(I) coordination polymer based on pyridyl-functionalized resorcin[4]arene: selective detection of $Cr_2O_7^{2-}$, MnO_4^- and nitrobenzene and efficient catalyst for azide-alkyne cycloaddition reaction

Yan-Li Liu,[a] Lei Yan,[b] Ying-Ying Liu,[a,*] Guo-Hai Xu,[c,*] Wen-Jing Shi,[d] and Jian-Fang Ma,[a,*]

[a]*Key Lab of Polyoxometalate Science, Department of Chemistry, Northeast Normal University, Changchun 130024, P. R. China*

[b]*School of Chemistry, Dalian University of Technology, Dalian, Liaoning 116024, China*

[c]*Key Laboratory of Jiangxi University for Functional Materials Chemistry, School of Chemistry and Chemical Engineering, Gannan Normal University, Ganzhou, Jiangxi 341000, China*

[d]*School of Chemistry and Chemical Engineering, Guangzhou University, Guangzhou 510006, China*

* Correspondence authors

E-mail: liuyy147@nenu.edu.cn

E-mail: xugh308@gnnu.cn

E-mail: majf247@nenu.edu.cn

Fax: +86-431-85098620 (J.-F. Ma)

ABSTRACT

In this work, a novel Cu(I) coordination polymer, Cu_2LBr_2 (**1**) based on a pyridyl-functionalized resorcin[4]arene [L = (2,8,14,20-tetraethyl-4,10,16,22-tetra

kis((2-pyridylmethylene)oxy)-6,12,18,24-tetramethoxy-resorcin[4]arene)] has been synthesized under solvothermal condition. **1** was characterized by various physicochemical analyses and it shows a ribbon structure. Notably, **1** exhibits an outstanding thermal stability. **1** possesses strong luminescent property, and can selectively probe $Cr_2O_7^{2-}$, MnO_4^- and nitrobenzene via luminescent quenching. In addition, **1** is an efficient catalyst for azide-alkyne cycloaddition reaction.

Keywords: Copper(I), Resorcin[4]arene, Coordination polymer, Luminescence, Azide–alkyne cycloaddition

1. Introduction

Resorcin[4]arenes have emerged as a kind of excellent organic hosts with bowl-shaped cavities, and their rims could be modified by various functional groups [1,2]. Coordination polymers (CPs) based on resorcin[4]arene have aroused interest because of fascinating structures and diverse applications [3,4].

CPs as an important class of substances have been used in comprehensive fields such as gas adsorption, catalysis, luminescene, drug delivery, and so on [5-9]. In this respect, CPs-based luminescent quenching has drawn attention due to its selectivity, sensitivity and convenience [10,11]. It is well known that $Cr_2O_7^{2-}$ and MnO_4^- are common and important oxidants in both laboratory and industry [12]. $Cr_2O_7^{2-}$ anion has caused serious pollution towards ecological environment and threatened the survival of various creatures because of its widely usage [13,14]. Also, nitrobenzene (NB) as one of the poisonous organic pollutants has been utilized extensively in dyes, anilines, explosives and pesticides [15,16]. Although a few multiple analytes have been reported to probe their existence, it is still pressing to explore and develop new efficient sensor [17-19].

CPs as heterogeneous catalysts possess many advantages compared to conventional homogeneous catalysts, such as selectivity, easy separation, and high catalytic performance [20,21]. Azide–alkyne cycloaddition (AAC) known as “click” reaction can be catalyzed via Cu(I)-CPs to generate 1,4-disubstituted 1,2,3-triazoles [22]. Much attention has been paid to this reaction owing to its inherent advantages

such as procedural simplicity, high selectivity and ultrahigh conversion [23]. In this regard, various Cu(I)-CPs have been explored as effective catalysts with perfect yields and regioselectivity for AAC reactions [24-26].

In view of the luminescent and catalytic properties, a Cu(I)-based CP, Cu_2LBr_2 (**1**), was achieved by a novel pyridyl-functionalized resorcin[4]arene (2,8,14,20-tetraethyl-4,10,16,22-tetrakis((2-pyridylmethylene)oxy)-6,12,18,24-tetram ethoxy-resorcin[4]arene) (L). Its structure was judged by crystallographic data and a series of physical characterizations. It is worth noting that **1** can be used as luminescent sensor to detect $Cr_2O_7^{2-}$, MnO_4^- and NB with high selectivity. Furthermore, **1** shows excellent catalytic activities for AAC reaction.

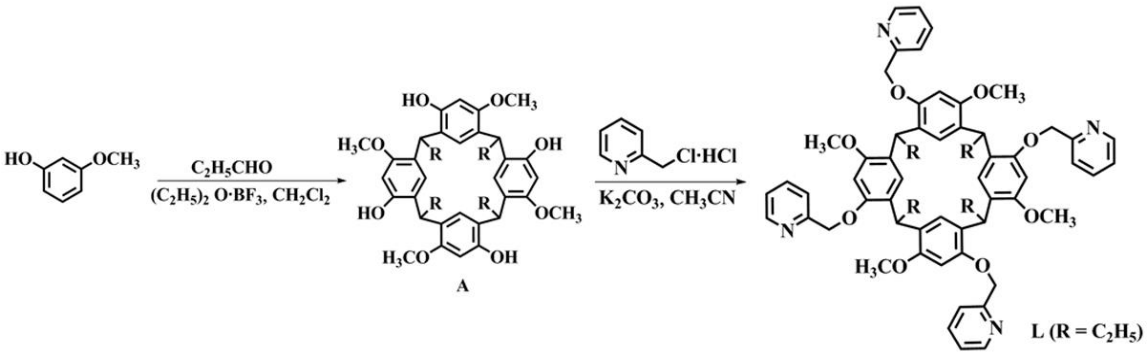

Scheme 1. Synthetic route of L.

2. Experimental

2.1. Materials and instruments

IR spectra were gained by an Alpha Centaurt FT/IR spectrophotometer. TGA was measured by a Perkin-Elmer TG-7 analyzer at a rate of 10 °C/min under N_2 atmosphere. PXRD patterns were performed on a Rigaku Dmax 2000 X-ray diffractometer with Cu-Kα radiation (λ = 0.154 nm). The catalytic yields of AAC reaction were confirmed via GC equipment which is equipped with a FID detector (GC-2014C, Shimadzu, Japan) and a capillary (30 m × 0.25 mm, WondaCAP 17). ^1H NMR spectra were determined in $CDCl_3$ on a Bruker 600 MHz. The luminescent data were collected by an Edinburgh FLSP920 fluorescence spectrometer, with Xenon flash lamp, scan slit of 1.00 nm, Dwell time of 0.10 s and step of 1.00 nm. Solid state UV–vis absorption spectra were obtained by a Cary 500 spectrophotometer. The morphology was gained by a HITACHI SU8010 scanning electron microscope.

2.2. X-ray crystallography

Crystallographic data of **1** was collected by an Oxford Diffraction Gemini R CCD diffractometer using Mo-Kα radiation (λ = 0.71073 Å). The refinement of the structure was solved by the method of full-matrix least-squares using SHELXL-2013 program. The elaborate crystal data were listed in Tables 1 and 2.

2.3. Synthesis of L

The intermediate A (2,8,14,20-tetra-ethyl-4,10,16,22-tetra-hydroxy-6,12,18,24-tetra-methoxy-resorcin[4]arene) was prepared according to previous report [27]. The mixture of A (5.60 g, 8.52 mmol), K_2CO_3 (14.62 g, 0.106 mol) and 500 mL acetonitrile was stirred for 0.5 h at rt. After that, 2-picolyl chloride hydrochloride (8.69 g, 0.053 mol) was added into the mixture gradually. The reactive solution was heated to reflux for 30 h under N_2 atmosphere. The solvent was removed by rotary evaporation and the obtained solid was washed by water. The white solid was recrystallized with CH_2Cl_2 and MeOH and then dried (yield = 89.65%) (Scheme 1). IR (cm^{-1}): 3669 (w), 3063 (w), 2959 (m), 2931 (m), 2832 (w), 1608 (m), 1591 (s), 1496 (s), 1444 (m), 1375 (w), 1302 (s), 1197 (s), 1160 (m), 1122 (s), 1049 (m), 814 (w), 755 (m), 401 (w) (Fig. S1).

*2.4. Synthesis of Cu_2LBr_2(**1**)*

$CuBr_2$ (8 mg, 0.036 mmol), L (10 mg, 0.01 mmol) and water/MeOH (6/2 mL) was sealed in a 15 mL reactor and the temperature was kept at 160°C for 24 h. Then it was slowly cooled to ambient temperature. The afforded yellow rod crystals of **1** were washed with water/methanol (3:1 V/V) thoroughly and air-dried (based on L yield: 54%). Anal. Calcd for $C_{64}H_{68}N_4O_8Cu_2Br_2$: C, 58.71; H, 5.19; N, 4.28. Found: C, 58.53; H, 5.39; N, 4.36. IR (cm^{-1}): 3068 (w), 2958 (m), 2830 (w), 1507 (s), 1436 (m), 1385 (m), 1299 (s), 1197 (s), 1123 (m), 1047 (m), 810 (w), 766 (w), 520 (w), 414(w).

2.5. Procedure of luminescent sensing

Ground **1** (3 mg) was immersed in 3 mL various aqueous solutions containing different anions or organic solvents respectively. The mixtures were treated via ultrasonic agitation to yield suspensions. The luminescent intensities were detected by using the acquired suspensions.

2.6. Procedure for AAC reaction

In a 15 mL pressure-proof pipe, alkynes (2 mmol), azides (1 mmol), **1** (10 mg, 0.0076 mmol), amyl acetate (0.92 mmol) and MeOH (4 mL) were added. The

obtained mixture was stirred at 80°C for 12 h. Herein, amyl acetate was used as internal standard reagent. The products of the catalytic reactions were confirmed by ^{1}H NMR (Fig. S6). The final conversions were calculated by GC (Figs. S7 and S8).

Table 1. Crystallographic data of **1**.

Formula	$C_{64}H_{68}Br_2Cu_2N_4O_8$
Mr	1308.12
Crystal system	Monoclinic
Space group	*C*2/*c*
a(Å)	25.385 (2)
b(Å)	16.408 (17)
c(Å)	18.629 (2)
α(°)	90
β(°)	130.593 (10)
γ(°)	90
V(Å^3)	5892 (1)
Z	4
T(K)	293
D_{calc} (g cm^{-3})	1.475
F(000)	2688
R_{int}	0.0626
GOF on F^2	0.989
$R_1{}^a$ [I>2σ(I)]	0.0634
$wR_2{}^b$ (all data)	0.0986

$^aR_1 = \Sigma||F_o| - |F_c||/\Sigma|F_o|$. $^bwR_2 = \{\Sigma[w(F_o^2-F_c^2)^2]/\Sigma w(F_o^2)^2]\}^{1/2}$.

Table 2. Selected bond distances (Å) and angles (deg) for **1**.

Cu(1)-N(3)$^{\#1}$	2.084(4)	N(3)$^{\#1}$-Cu(1)-N(1)	103.74(15)
Cu(1)-N(1)	2.108(4)	N(3)$^{\#1}$-Cu(1)-Br(1)	105.79(12)
Cu(1)-Br(1)	2.5125(11)	N(1)-Cu(1)-Br(1)	125.69(12)
Cu(1)-Br(1)$^{\#2}$	2.5448(11)	N(3)$^{\#1}$-Cu(1)-Br(1$^{\#2}$	120.54(12)
Br(1)-Cu(1)-Br(1)$^{\#2}$	104.56(3)	N(1)-Cu(1)-Br(1)$^{\#2}$	97.97(12)

Symmetry codes: $^{\#1}$ x, -y, z + 1/2, $^{\#2}$ -x, y, - z + 1/2.

3. Results and discussion

*3.1. Crystal Structure of **1***

The independent unit of **1** consists of one Cu(I) ion, half of L and one Br^- anion. Each Cu(I) coordinates with two pyridyl nitrogen atoms from two L ligands and two Br^- anions, developing a tetrahedral coordination geometry. All nitrogen atoms in L are participating in the coordination (Fig. 1a). The orientations of the pyridyl rings in L are different. Each Br^- anion acts as a bridging node and connects two adjacent Cu(I) ions to produce a di-Cu(I) unit. L ligands connect dinuclear units to form a ribbon (Fig. 1b).

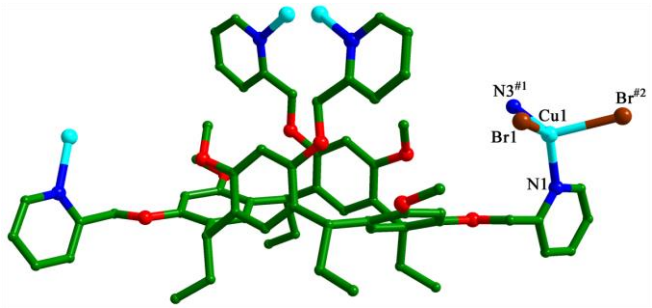

(a)

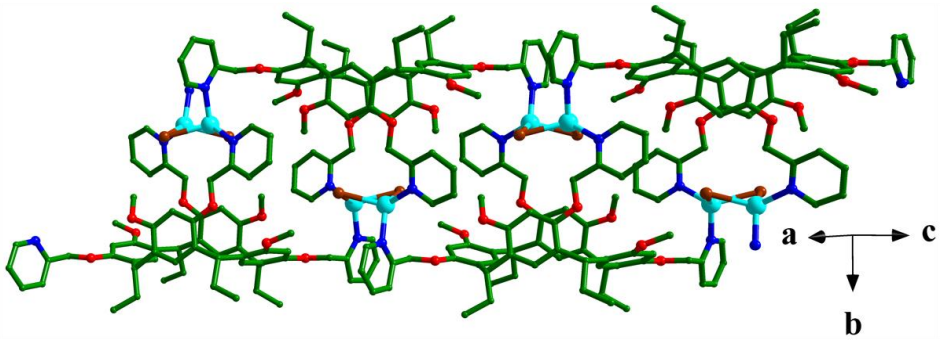

(b)

Fig. 1. (a) Coordination spheres of Cu(I) and L (Symmetry codes: #1x, -y, z + 1/2; #2-x, y, -z + 1/2). (b) View of the ribbon.

3.2. Thermal and Chemical Stability.

To explore the thermal stability, thermogravimetric measurement was conducted (Fig. 2). For **1**, no marked change before 304°C was detected. This implies its superior thermal stability. After that, the framework began to collapse.

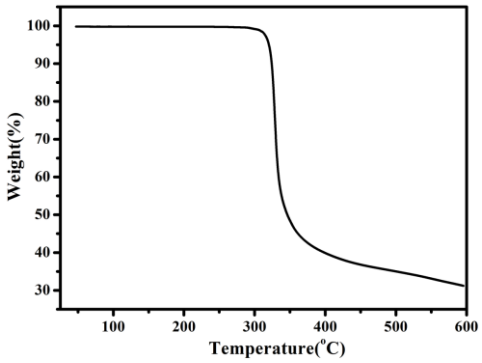

Fig. 2. TG curve of **1** recorded in N_2 atmosphere.

In order to investigate the chemical stability, **1** (20 mg) was soaked in water solutions (10 mL) with different pH values ranging from 2 to 13, and various organic solvents (10 mL) including dichloromethane (DCM), acetonitrile (MeCN), cyclohexane (CYH), dimethylforamide (DMF), acetone, methanol (MeOH) and ethanol (EtOH) for 24 h, respectively. As depicted in Fig. 3, almost all of the PXRD curves match well with the simulated one, except that there is an additional peak at 2θ = 13.6° in several curves. This demonstrates that the frameworks remained unchanged [28]. After filtering the above mixtures, three filtrates (treated by pH = 2, pH = 13 and DCM) were selected to test the dissolubility of **1** by ICP. The Cu(I) contents are 33.06, 42.56 and 0 μg, respectively. The results showed that **1** has faint solubility in strong acid or strong alkali solutions. The additional peaks in several PXRD curves may be influenced by the solvation or the different interplanar orientation of the crystals.

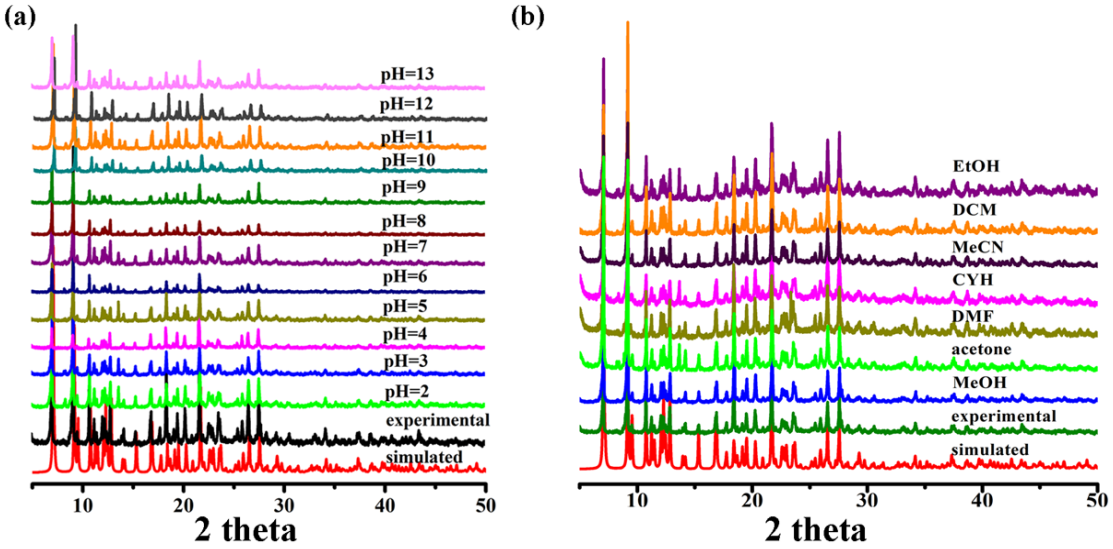

Fig. 3. PXRD curves of **1** immersed in water solutions with different pH values (a), and various organic solvents (b).

3.3. Luminescent property

As demonstrated in Fig. 4, L shows an emission at 447 nm (λ_{ex} = 380 nm), which is due to $\pi^*\rightarrow n$ or $\pi^*\rightarrow\pi$ transitions [29]. The stronger emission peak of **1** occurs at 576 nm (λ_{ex} = 380 nm), which is red shifted by 129 nm with respect to L. According to previous report, the emission of **1** is originated from the metal-to-ligand charge-transfer [30]. The luminescent intensity of **1** displays an obvious increase over L, which may be attributed to the reinforce of the rigidity of the coordination between L and Cu(I) ions [31].

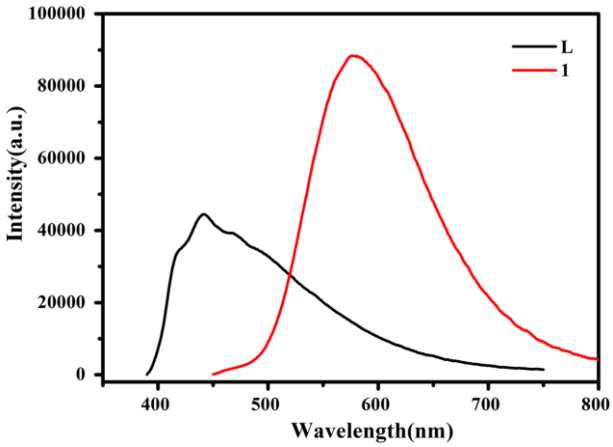

Fig. 4. Solid state luminescent spectra of L and **1**.

The temperature-dependent emission spectrum of **1** is revealed under liquid nitrogen. Along with the temperature rising from 90 to 290 K, the emission peaks show a slight blue shift from 604 nm to 588 nm. Meanwhile, the emission intensities decreased (Fig. S2). The increment of intensities under cryogenic condition is due to reducing the loss of energy via nonradiative decay [32].

3.4. Sensing of $Cr_2O_7^{2-}$ and MnO_4^-

Considering the strong luminescent intensity of **1**, its underlying application in detecting anions was performed systematically. In this work, ground finely **1** (3 mg) was soaked in 3 mL aqueous solutions including K_nX (0.01 M, X = OH^-, Br^-, Cl^-, I^-, SCN^-, $S_2O_8^{2-}$, HCO_3^-, SO_4^{2-}, CO_3^{2-}, $Cr_2O_7^{2-}$ and MnO_4^-). As illustrated in Fig. 5, the emissions of **1** are largely related to the anionic species. Apparently, $Cr_2O_7^{2-}$ and MnO_4^- display obvious quenching compared to other anions.

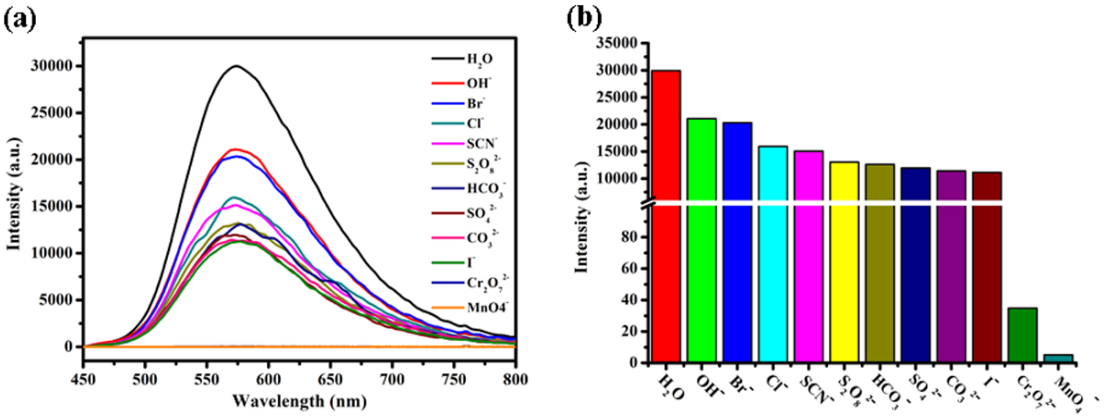

Fig. 5. Emission spectra (a) and intensities (b) of **1** in various anionic aqueous solutions (λ_{ex} = 380 nm).

In order to measure the ability of anti-interference of **1** towards anions, competitive experiment was operated by taking $Cr_2O_7^{2-}$ as an example. Finely mulling **1** (3 mg) was immersed in a series of aqueous solutions containing $Cr_2O_7^{2-}$ (0.005 M) along with other anions (0.01 M) respectively. As illustrated in Fig. 6, the quenching effect of $Cr_2O_7^{2-}$ on **1** is still ultrahigh even though other anions are loaded. The phenomenon signifies excellent anti-interferential detecting ability of **1** towards $Cr_2O_7^{2-}$.

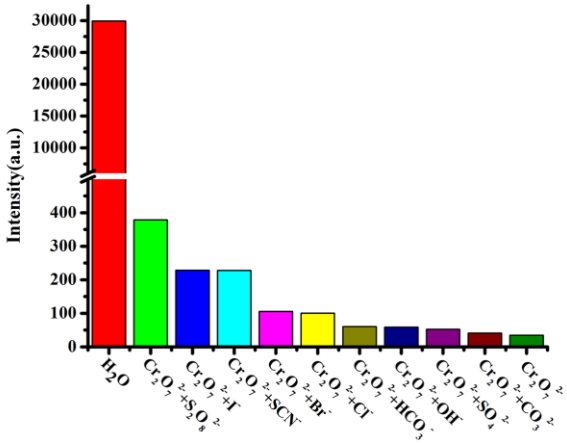

Fig. 6. Luminescent intensities of **1** with addition of $Cr_2O_7^{2-}$ and other anions (λ_{ex} = 380 nm).

3.5. Sensing of NB.

Organic toxic pollutants spread in water resource due to their widely usage in various fields [33]. Herein, **1** was utilized to detect small organic molecules via luminescent property. Fully ground **1** (3 mg) was immersed in 3 mL pure organic

solvents (MeCN, MeOH, acetone, EtOH, 2-propanol (IPA), DMF, DCM, DMA or NB). As depicted in Fig. 7, all luminescent intensities in various solvents except NB reach up to great counts. That is, NB exhibits an obvious quenching effect.

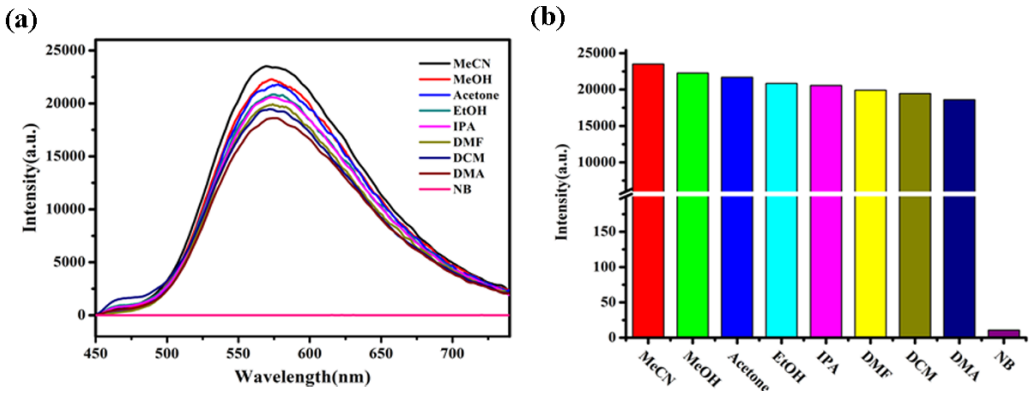

Fig. 7. Emission spectra (a) and intensities (b) of **1** in different organic solvents.

To evaluate the anti-interference test of **1** for NB, the suspension of **1** (3 mg) with NB (1.5 mL) was introduced into other organic solvents (1.5 mL). As depicted in Fig. 8, the emission intensities of **1** in mixed solvents are much lower than those in pure solvents. That is, the quenching selectivity of **1** on NB was not influenced by the presence of other solvents.

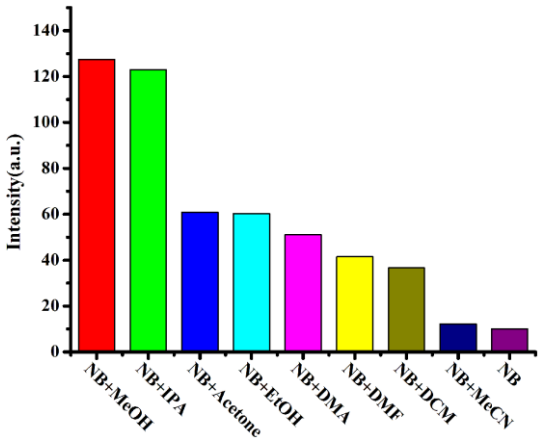

Fig. 8. Luminescent intensities of **1** in mixed solvents consisting of equal NB and other organic solvents.

In order to study the recyclable performance of **1** in quenching, the reusability tests of **1** were studied. After three runs of sensing $Cr_2O_7^{2-}$ or NB, their quenching efficiencies only decreased about 1% (Fig. S3), which imply that **1** processes an excellent recyclability.

To analyse the mechanism of quenching, **1** (20 mg) was immersed in the aqueous solutions of $Cr_2O_7^{2-}$ (0.01 M, 20 mL) or NB (20 mL) for 24 h. Their main PXRD

peaks are identical to that of the simulated pattern, which illustrate that the basic framework of **1** remains unchanged (Fig. S4). Then the solid state UV-vis spectra of L and **1** were tested. There is an intensive absorption band from 200 to 475 nm for **1** (Fig. S5). Strong absorptions could be observed for the solution of $Cr_2O_7^{2-}$ (ranging from 250 to 450 nm) and NB (ranging from 225 and 320 nm), which are within the band scope of **1** [34]. Upon excitation, $Cr_2O_7^{2-}$ or NB competes with **1** for absorption energy, thus resulting in the luminescent quenching [35,36].

3.6. Catalytic performance

Cu(I)-CPs are fascinating not only for their luminescent properties, but also for their catalytic effects in AAC reactions [37]. To optimize the reactive condition, phenylacetylene and benzyl azide were conducted as the model substrates with different loadings of **1** under diverse temperatures and solvents (Table 3, Fig. S7). Under MeOH solvent and 80 °C, the conversions were elevated from 6% to 98% and 99% with increasing loadings of **1** from 0 to 10 and 15 mg for 12 h (entries 1-4). Subsequently, the reactions were done at 40°C and 60°C with catalyst **1** (10 mg) to identify the suitable temperature. Only 14% and 72% yields were obtained respectively (entries 5-6). In order to explore the effects of solvents, the reactions were operated in different organic solvents containing MeCN, DCM and EtOH. The best yields of 98% compared to those in MeCN and DCM can be gained in MeOH and EtOH (entries 7-9).

Table 3. The catalytic reactions of phenylacetylene and benzyl azide under different conditions [a].

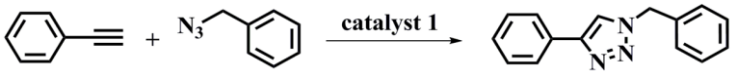

entry	Catalyst (mg)	Temperature (°C)	Solvent	Yield[b] (%)
1	0	80	MeOH	6%
2	5			88%
3	10			98%
4	15			99%

5	10	40		14%
6		60		72%
7		80	MeCN	58%
8			DCM	64%
9			EtOH	98%

[a]Reactive conditions: phenylacetylene (204 mg, 2mmol), benzyl azide (133 mg, 1 mmol) and amyl acetate (120 mg, 0.92 mmol). [b]Amyl acetate was used to calculate the yield by GC.

Under the optimized condition (10 mg of **1**, MeOH and 80°C), kinetic experiment between phenylacetylene and benzyl azide was tested to trace the reactive progress. As shown in Table 4 and Figs. S7 and S9, the yield increased rapidly to 90% after 8 h. Then, it continued to rise slowly from 90% to 98% in the following 4 h.

Table 4. The effects of time on the catalytic reactions of benzyl azide and phenylacetylene.

entry	Catalyst (mg)	Temperature (°C)	Solvent	Time (h)	Yield (%)
1	10	80	MeOH	2	36%
2				6	86%
3				8	90%
4				10	93%
5				12	98%

The next study focused on the catalytic universality of **1**. Under the optimal condition (10 mg of **1**, MeOH, 80°C and 12 h), the reactions between functionalized benzyl azides and phenylacetylenes were studied (Table 5 and Fig. S8). For para- and meta-CH_3 substituted benzyl azide, slightly lower yields (90% and 94%) were gained (entries 2-3). When benzyl azide was substituted by other functional groups (ortho-F, meta-NO_2 and para-CN), the conversion yields can reach to 99% or 98%, respectively (entries 4-6). Several substituted phenylacetylenes (para-F, -Cl, -methyl and -methoxy) were also tried to react with benzyl azide and all yields can reach up to 98% or 99%

(entries 7-10). The high yields of above experiments implied that **1** owns excellent catalytic universality for AAC reaction.

Table 5. Catalytic reactions of benzyl azides and phenylacetylenes with various functional groups[a].

entry	Azide	Alkyne	Product	Yield(%)
1	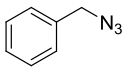	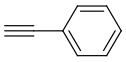	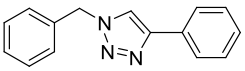	98%
2	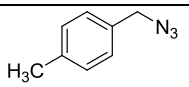		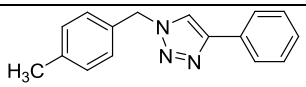	90%
3	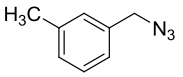		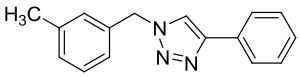	94%
4	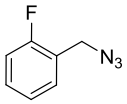		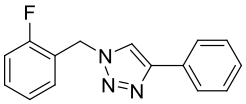	99%
5	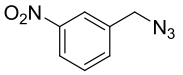		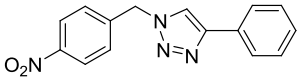	98%
6	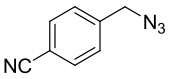		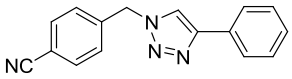	98%
7	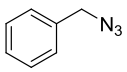	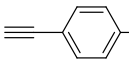	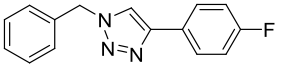	98%
8		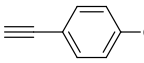	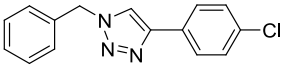	99%
9		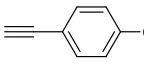	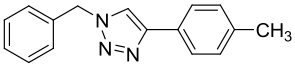	98%
10		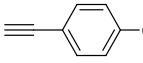	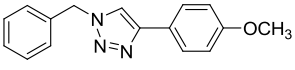	98%

[a]Reactive conditions: alkynes (2 mmol), azides (1 mmol), amyl acetate (0.92 mmol), **1** (10 mg, 0.0076 mmol) and methanol (4 mL) at 80℃ for 12 hours.

As to the catalytic reaction of 1-benzyl-4-phenyl-1H-1,2,3-triazole, **1** shows a higher yield in a more wider scope of substrates than those related CPs, such as Cu_3(BTC) (BTC = 1,3,5-tricarboxybenzene) (yield = 88%) [38] and $[(CuI)_2\{ArS(CH_2)_3SAr\}_2]_n$ (Ar = 4-F-C_6H_4) (yield = 97%) [39]. As to [CuBr(DAPTA)$_3$] (DAPTA = 3,7-diacetyl-1,3,7-triaza-5-phosphabicyclo[3.3.1]nonane) (99%) [40], **1** exhibits a similar yield under more milder condition. This illustrates

that **1** could be employed as a promising catalyst for AAC reaction.

On the basis of literatures [41,42], a possible route for AAC reaction by **1** is proposed (Scheme 2). It is generally accepted that Cu(I) ion attacks the alkyne, the coordination intermediate A reinforces the acidity of terminal alkynyl hydrogen, which result in the generation of intermediate Cu(I)–acetylide B. Then, N5 and N3 atoms in azide attack the electrophilic Cu(I) and C2 atoms in B to give a six-membered Cu(I)-cycle C. Meanwhile, the metallacycle undergoes ring rearrangement to yield D. After that, with the break of Cu–C bond and the protonation of intermediate triazole, the product E and the catalyst **1** are formed.

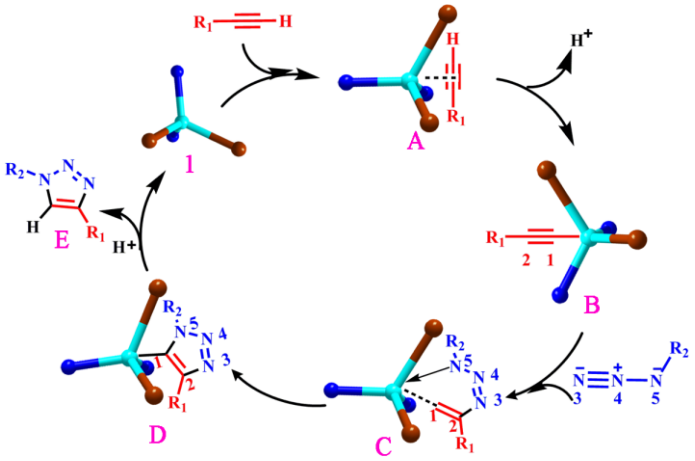

Scheme 2. Proposed mechanism for AAC reaction by **1**.

4. Conclusions

In brief, a novel Cu(I)-CP based on pyridyl-functionalized resorcin[4]arene has been prepared successfully. **1** displays a charming ribbon structure. **1** possesses an outstanding thermal stability. Systematical luminescent studies show that luminescent intensities of **1** are closely related to the types of anions and organic solvents. **1** can be used to probe $Cr_2O_7^{2-}$, MnO_4^- and NB with high selectivity. Remarkably, **1** can be employed as an excellent catalyst for AAC reaction with high activity and yield. Thus, **1** shows promising applications in both luminescent sensing and catalyst.

Acknowledgments

This work was supported by the National Natural Science Foundation of China (Grant No. 21471029 and 21761003). The Foundation for Distinguished Young Talents in

Higher Education of Guangdong (No. 2016KQNCX119). Scientific Research Project of Guangzhou Municipal Colleges and Universities (No. 1201630192).

References

[1] R.S. Patil, H. Kumari, C.L. Barnes, J.L. Atwood, Chem. Commun. 51 (2015) 2304.

[2] W.-Y. Pei, G.H. Xu, J. Yang, H. Wu, B.L. Chen, W. Zhou, J.-F. Ma, J. Am. Chem. Soc. 139 (2017) 7648.

[3] Y.-J. Hu, J. Yang, Y.-Y. Liu, S.Y. Song, J.-F. Ma, Cryst. Growth Des. 15 (2015) 3822.

[4] P. P. Cholewa, S.J. Dalgarno, CrystEngComm. 16 (2014) 3655.

[5] R.-W. Huang, Y.-S. Wei, X.-Y. Dong, X.-H. Wu, C.-X. Du, S.-Q. Zang, T.C.W. Mak, Nat. Chem. 9 (2017) 689.

[6] T.-T. Wang, J.-L. Zhang, H.-M. Hu, Y. Cheng, L.-L. Xue, X.F. Wang, B.-Z. Wang, Polyhedron 151 (2018) 43.

[7] H.-Y. Li, Y.-L. Wei, X.-Y. Dong, S.-Q. Zang, T.C.W. Mak, Chem. Mater. 27 (2015) 1327.

[8] B.L. Martinez, A.D. Shrode, R.J. Staples, R.L. LaDuca, Polyhedron 151 (2018) 369.

[9] X.-Y. Dong, R. Wang, J.-Z. Wang, S.-Q. Zang, T.C.W. Mak, J. Mater. Chem. A 3 (2015) 641.

[10] J.W. Ye, L.M. Zhao, R.F. Bogale, Y. Gao, X.X. Wang, X.M Qian, S. Guo, J.Z. Zhao, G.L. Ning, Chem. Eur. J. 21 (2015) 2029.

[11] X.-J. Jiang, M. Li, H.-L. Lu, L.-H. Xu, H. Xu, S.-Q. Zang, M.-S. Tang, H.-W. Hou, T.C.W. Mak, Inorg. Chem. 53 (2014) 12665.

[12] M. Chen, W.-M. Xu, J.-Y. Tian, H. Cui, J.-X. Zhang, C.-S. Liu, M. Du, J. Mater. Chem. C 5 (2017) 2015.

[13] J.-Y. Zou, L. Li, S.-Y. You, H.-M. Cui, Y.-W. Liu, K.-H. Chen, Y.-H. Chen, J.-Z. Cui, S.-W. Zhang, Dyes Pigments 159 (2018) 429.

[14] L. Zhao, J. Zhang, J. Wang, X.-Y. Niu, X.-Q. Wang, L.-M. Fan, T.-P. Hu, J. Soild State Chem. 268 (2018) 1.

[15] B.B. Liu, X.L. Lin, H. Li, K.X. Li, H. Huang, L. Bai, H.L. Hu, Y. Liu, Z.H. Kang, Cryst. Growth Des. 15 (2015) 4355.

[16] L.-L. Liu, J. Chen, C.-X. Yu, W.-X. Lv, H.-Y. Yu, X.-Q. Cui, L. Liu, Dalton Trans. 46 (2017) 178.

[17] C.-S. Cao, H.-C. Hu, H. Xu, W.-Z. Qiao, B. Zhao, CrystEngComm. 18 (2016) 4445.

[18] Y.-T. Yan, F. Cao, W.-Y. Zhang, S.-S. Zhang, F. Zhang, Y.-Y. Wang, New J. Chem. 42 (2018) 9865.

[19] R.-M. Wen, S.-D. Han, G.-J. Ren, Z. Chang, Y.-W. Li, X.-H. Bu, Dalton Trans. 44 (2015) 10914.

[20] J. Chai, P.C. Wang, J. Jia, B. Ma, J. Sun, Y.F. Tao, P. Zhang, L. Wang, Y. Fan, Polyhedron 141 (2018) 369.

[21] J. Xia, J.N. Xu, Y. Fan, T.Y. Song, L. Wang, J.F. Zheng, Inorg. Chem. 53 (2014) 10024.

[22] L.Y Liang, D. Astruc, Coordin. Chem. Rev. 255 (2011) 2933.

[23] D. Mendoza-Espinosa, G.E. Negrón-Silva, D. Ángeles-Beltrán, A. Álvarez-Hernández, O.R. Suárez-Castillo, R. Santillán, Dalton Trans. 43 (2014) 7069.

[24] W. Jiang, J. Yang, Y.-Y. Liu, J.-F. Ma, Chem. Commun. 52 (2016) 1373.

[25] B.-B. Lu, J. Yang, G.-B. Che, W.-Y. Pei, J.-F. Ma, ACS Appl. Mater. Inter. 10 (2018) 2628.

[26] F. Himo, T. Lovell, R. Hilgraf, V.V. Rostovtsev, L. Noodleman, K.B. Sharpless, V.V. Fokin, J. Am. Chem. Soc. 127 (2005) 210.

[27] K.-X. Chang, N. Zhang, P. Du, Y.-Y. Liu, J.-F. Ma, Polyhedron 138 (2017) 287.

[28] Y. Wang, N. Du, X. Zhang, Y. Wang, Y.-H. Xing, F.-Y. Bai, L.-X. Sun, Z. Shi, Cryst. Growth Des. 18 (2018) 2259.

[29] S.-T. Zhang, J. Yang, H. Wu, Y.-Y. Liu, J.-F. Ma, Chem. Eur. J. 21 (2015) 15806.

[30] C.M. Brown, V. Carta, M.O. Wolf, Chem. Mater. 30 (2018) 5786.

[31] Q.-W. Guan, D. Zhang, Z.-Z. Xue, X.-Y. Wan, Z.-N. Gao, X.-F. Zhao, C.-P. Wan, J. Pan, G.-M. Wang, Inorg. Chem. Commun. 95 (2018) 144.

[32] B. Li, R.-W. Huang, J.-H. Qin, S.-Q. Zang, G.-G. Gao, H.W. Hou, Thomas C. W. Mak, Chem. Eur. J. 20 (2014) 12416.

[33] S.-Q. Lu, Y.-Y. Liu, Z.-M. Duan, Z.-X. Wang, M.-X. Li, X. He, Cryst. Growth Des. 18 (2018) 4602.

[34] S.-S. Jin, X. Han, J. Yang, H.-M. Zhang, X.-L. Liu, J.-F. Ma, J. Lumin. 188 (2017) 346.

[35] Y.-P. Xia, C.-X. Wang, R. Feng, K. Li, Z. Chang, X.-H. Bu, Polyhedron 153 (2018) 110.

[36] X.-J. Liu, X. Wang, J.-L. Xu, D. Tian, R.-Y. Chen, J. Xu , X.-H. Bu, Dalton Trans. 46 (2017) 4893.

[37] M. Meldal, C.W. Tornøe, Chem. Rev. 108 (2008) 2952.

[38] X.R. Jia, G.L.Xu, Z.Y. Du, Y. Fu, Polyhedron 151 (2018) 515.

[39] S. Saha , K. Biswas, B. Basu, Tetrahedron Lett. 59 (2018) 2541.

[40] A.G. Mahmoud, M.F.C. Guedes da ilva, J. Sokolnicki, P. Smoleński , A.J.L. Pombeiro, Dalton Trans. 47 (2018) 729.

[41] Y. Zhou, T. Lecourt, L. Micouin, Angew. Chem. Int. Ed. 49 (2010) 2607.

[42] M. Amini, S. Najafi, J. Janczak, Inorg. Chim. Acta. 482 (2018) 333.

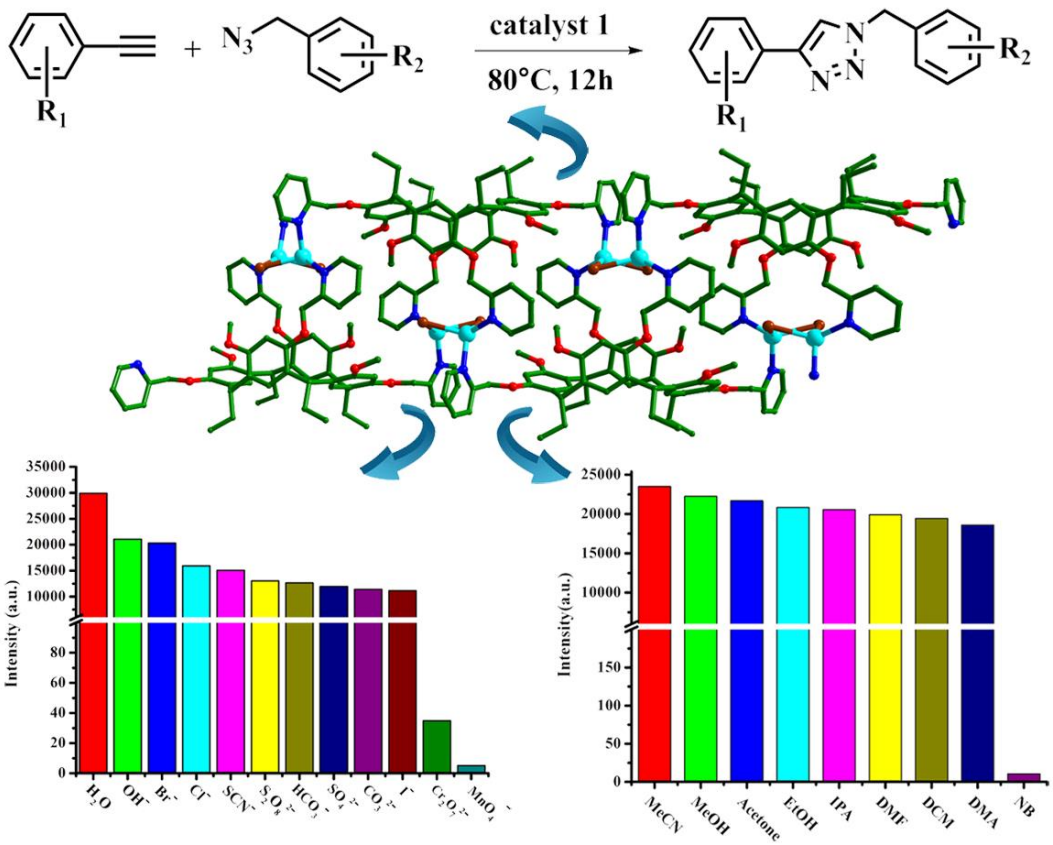
catalyst 1
80°C, 12h
R1
R2
N3
Intensity (a.u.)
Intensity(a.u.)
MeCN
MeOH
Acetone
EtOH
IPA
DMF
DCM
DMA
NB

In this work, a Cu(I) coordination polymer constructed by a novel pyridyl-functionalized resorcin[4]arene and $CuBr_2$ has been synthesized and structurally characterized. It can selectively detect $Cr_2O_7^{2-}$, MnO_4^- and nitrobenzene via luminescent quenching and effectively catalyse azide-alkyne cycloaddition reaction.